



Full length article

Study of in-situ formation of Fe-Mn-Si shape memory alloy welding seam by laser welding with filler powder



Heng Ju, Chengxin Lin*, Zhijie Liu, Jiaqi Zhang

Transportation Equipment and Ocean Engineering College, Dalian Maritime University, Dalian 116026, China

ARTICLE INFO

Article history:

Received 25 September 2017

Received in revised form 28 December 2017

Accepted 29 January 2018

Keywords:

Laser welding

Filler powder

Restrained mixing uniform design method

Fe-Mn-Si shape memory alloy welding seam

Mechanical properties

Stress-induced $\gamma \rightarrow \varepsilon$ martensite transformation

ABSTRACT

To reduce the residual stresses and improve the mechanical properties of laser weldments, produced with the restrained mixing uniform design method, a Fe-Mn-Si shape memory alloy (SMA) welding seam was formed inside the 304 stainless steel by laser welding with powder filling. The mass fraction, shape memory effect, and phase composition of the welding seam was measured by SEM-EDS (photometric analyser), bending recovery method, and XRD, respectively. An optical microscope was used to observe the microstructure of the Fe-Mn-Si SMA welding seam by solid solution and pre-deformation treatment. Meanwhile, the mechanical properties (residual stress distribution, tensile strength, microhardness and fatigue strength) of the laser welded specimen with an Fe-Mn-Si SMA welding seam (experimental material) and a 304 stainless steel welding seam (contrast material) were measured by a tensile testing machine hole drilling method and full cycle bending fatigue test. The results show that Fe15Mn5Si12Cr6Ni SMA welding seam was formed in situ with shape memory effect and stress-induced $\gamma \rightarrow \varepsilon$ martensite phase transformation characteristic. The residual stress of the experimental material is lower than that of the contrast material. The former has larger tensile strength, longer elongation and higher microhardness than the latter has. The experimental material and contrast material possess 249 and 136 bending fatigue cycles at the strain of 6%, respectively. The mechanisms by which mechanical properties of the experimental material are strengthened includes (1) release of the residual stress inside the Fe-Mn-Si SMA welding seam due to the stress-induced $\gamma \rightarrow \varepsilon$ martensite phase transformation and (2) energy absorption and plastic slip restraint due to the deformations in martensite and reverse phase transformation.

© 2018 Elsevier Ltd. All rights reserved.

1. Introduction

Laser welding has been widely used for its conspicuous advantages in narrowly focusing laser radiation providing high intensity heat source, fast processing efficiency and good metallurgical bonding [1–5]. However, the processing possesses some negative characteristics, as follows: (1) the small beam size and the fast heating and cooling speed of the laser and (2) the low thermal conductivity and high expansion coefficient of welding materials. The high residual tensile stress and hot crack also exist in the laser weldment, which can create some defects including decreased stability, degraded and stiffness [6]. In addition, 90% of the failure in the service period of laser welded assembly is caused by fatigue break [7]. Thus, it is necessary to release the welding residual stress and improve the fatigue characters of the laser weldment. Presently, new technology of laser welding with powder filler

can change the weld composition and refine the metal structure to improve welding performance [8–10]. A laser welding seam of low residual stress and high fatigue strength prepared by the new technology has practical significance.

As we all know, the SMAs (Ni-Ti-based, Cu-based and Fe-Mn-Si-based) possess shape memory effect, superelasticity, stress self-accommodation characteristic and so on [11,12]. Therein, superelasticity releases the stress concentration in the crack tip, and the crack growth is restrained to enhance the material strength. The stress self-accommodation characteristic can absorb energy and restrain plastic deformation to improve fatigue life of the materials. Oliveria et al. have researched the cycling behaviour of Ni-Ti SMA laser weldment and obtained the results that the welding specimen still has superelastic effect and stands 600 cycles at the strain of 10%. In addition, the heat affected and the fusion zone show martensite, and the stress relief phenomenon is observed for the principal stress in the base material [13,14]. Lin et al. have discussed the process of laser welding Fe-Mn-Si SMA, which shows the welding residual stress can also induce $\gamma \rightarrow \varepsilon$ martensite phase

* Corresponding author.

E-mail address: lxhxin@dlmu.edu.cn (C. Lin).

transformation, and the bending fatigue strength of welds reaches 90% of base metal [15]. Consequently, the weldment of SMA welding seam prepared by laser welding with filler powder would possess low residual stress and high fatigue strength in theory.

The 304 austenitic stainless steels have been used as nuclear structural materials for reactor coolant piping, valve bodies and vessel internals because of their excellent mechanical properties. Its applications also require the complex shapes jointed by laser welding process [16,17]. However, the laser welding process often degrades mechanical properties of stainless steel, and the above problem can be solved by the technology of laser welding with powder filling and the characteristic of SMA. After considering the consistency of powder and substrate, the Fe/Mn/Si/Cr/Ni mixed powder is selected as filler powder to inform the Fe-Mn-Si SMA welding seam. Judging by the tensile strength, the single factor experiment and orthogonal test were used to optimize technological parameters of the laser welding. Under the optimum process parameters, a stainless Fe15Mn5Si12Cr6Ni SMA welding seam was formed with the restrained mixing uniform design method. Its shape memory effect and stress-induced $\gamma \rightarrow \varepsilon$ martensite phase transformation characteristic are investigated. The filling material used is the material which possesses the same mass fraction as the welding substrate, so the 304 stainless steel powder was selected as contrast material. The residual stress distribution, tensile strength, microhardness and fatigue strength of the experimental material and contrast material are comparatively researched.

2. Experimental materials and methods

2.1. Materials and tensile test

The 304 stainless steel (chemical composition wt.%: Cr 18.14, Ni 8.71, Mn 1.148, Si, 0.404, C 0.069, Fe bal.) with dimensions of $100 \times 100 \times 2$ (mm) was used as the substrate material, and its groove size is $2 \text{ mm} \times 45^\circ$. The edges of the steel plates were ground and cleaned to ensure the dimension and the cleanliness of the substrate. The filler powders are Fe/Mn/Si/Cr/Ni homemade powder and 304 stainless steel powder, and they (particle sizes ranged from 45 to $100 \mu\text{m}$) were mixed by a QM-1 horizontal bowl mill for 4 h. The 1 mm-thick powders were pre-placed on the centre of the welding substrate after drying in a DZF-6030B vacuum drying oven at 150°C for 2 h. A DL-LPM-V CO_2 laser processing system with a maximum power of 5 Kw and a copper focusing lens with focal length of 300 mm were selected to get a 0.5 mm laser focusing spot. The schematic illustration of the laser welding is shown in Fig. 1.

The metallurgical bonding between substrate and powder is the precondition to prepare the Fe-Mn-Si SMA laser welding seam. Judging by the tensile strength, the optimum process parameters are first chosen with the preliminary single factor test and the orthogonal test. Table 1 shows the technological parameters of 15 tests in the single factor experiment. Samples 1#–5#, 6#–10#

Table 1
Process parameters of the single factor experiment in laser welding.

Number	Laser power, KW	Welding speed, mm/min	Defocusing amount, mm
1#	2.0	150	0
2#	2.2	150	0
3#	2.4	150	0
4#	2.6	150	0
5#	2.8	150	0
6#	2.4	100	0
7#	2.4	125	0
8#	2.4	150	0
9#	2.4	175	0
10#	2.4	200	0
11#	2.4	150	-5
12#	2.4	150	-2.5
13#	2.4	150	0
14#	2.4	150	2.5
15#	2.4	150	5

and 11#–15# studied the effect of laser power, welding speed and defocusing amount on the tensile strength, respectively.

According to the national standard GB/T 2651-2008, the laser weldments were cut into tensile samples (the dimension as Fig. 2 shows), and the loading speed in the tensile test is 2 mm/min by the material testing machine.

2.2. In situ formation of Fe-Mn-Si shape memory alloy welding seam

Using the restrained mixing uniform design method, the regression equation between the independent and dependent variables can be obtained from the uniform design table under the restrained condition [18]. Based on the pre-experiments, the ratio of Fe, Mn, Si, Cr, and Ni elements in the mixed powder (independent variables) are restrained as follows: $\text{Fe} + \text{Mn} + \text{Si} + \text{Cr} + \text{Ni} = 1$, $0 \leq \text{Fe} \leq 0.5$, $0.35 \leq \text{Mn} \leq 0.5$, $0.1 \leq \text{Si} \leq 0.2$, $0.01 \leq \text{Cr} \leq 0.05$, $0.01 \leq \text{Ni} \leq 0.05$. Considering the accuracy and efficiency, the U_7^4 (7^4) table is chosen as the uniform design table (seen in the Table 2). Based on the above conditions, the ratio of the powder elements under constraint conditions is calculated by the DPS data processing system (seen in the Table 3). Then, the powder is weighed by the analytical balance with the measuring accuracy of 0.0001 mg.

The mass fraction of Fe, Mn, Si, Cr, and Ni elements in the Fe-Mn-Si alloy welding seam (dependent variables) was detected three times, and the average was taken by the SUPRA55 SEM-EDS (photometric analyser).

2.3. Properties of the laser welding samples

The welding seam with dimension of $100 \times 2 \times 0.5$ (mm) is heating up to 350°C for the measurement of the shape recovery ratio, and the principle of the method is shown in Fig. 3 [19].

Meanwhile, the microstructure of the welding seam with solid solution ($1000^\circ\text{C} \times 1 \text{ h}$) and predeformation treatment was observed by an OLYMPUS G $\times 51$ optical microscope.

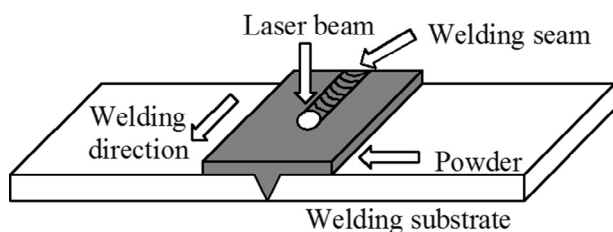


Fig. 1. Schematic illustration of laser welding.

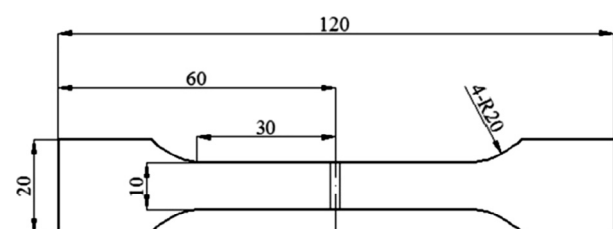


Fig. 2. Dimension of tensile sample (mm).

Download English Version:

<https://daneshyari.com/en/article/7128805>

Download Persian Version:

<https://daneshyari.com/article/7128805>

[Daneshyari.com](https://daneshyari.com)